

Route to ferromagnetism in organic polymers

Zsolt Gulácsi^{1,2}, Arno Kampf¹, and Dieter Vollhardt¹

¹ *Theoretical Physics III, Center for Electronic Correlations and Magnetism,
Institute of Physics, University of Augsburg, D-86135 Augsburg, Germany*

² *Department of Theoretical Physics,
University of Debrecen, H-4010 Debrecen, Hungary*

(Dated: November 14, 2018)

Abstract

Employing a rigorous theoretical method for the construction of exact many-electron ground states we prove that interactions can be employed to tune a bare dispersive band structure such that it develops a flat band. Thereby we show that pentagon chain polymers with electron densities above half filling may be designed to become ferromagnetic or half metallic.

PACS numbers: 71.10.Fd, 71.10.-w, 71.27.+a

Conducting polymers [1] are a fascinating class of materials with a strikingly wide range of applications, e.g., in nanoelectronics [2], nanooptics [3], and medicine [4]. Many of them contain chains of five-membered-rings as a building block. Such pentagon chain polymers have been explored [5, 6] and utilized [2] intensively in the past. In particular, polythiophene [7–9] was studied in the search for plastic ferromagnets and, more generally, for ferromagnetism in systems made entirely of nonmagnetic elements. The possibility for ferromagnetism in these systems was investigated theoretically [10, 11], with a particular focus on ferromagnetism due to flat electronic bands arising in odd-membered ring structures [12]. Particular attention was paid to the role of side groups of the pentagon ring, since these may cause flat bands in the band structure. Suwa *et al.* [13] proposed that ferromagnetism in pentagon-chain polymers such as polydimethylaminopyrrole is related to the hybridization of narrow σ bands with wide π bands and therefore modelled this polymer by a periodic Anderson model. In the latter model the electronic interaction acts site selective within the unit cell and the choice of this model [13] was an attempt to account for the different atoms on the pentagon chain.

In this Letter we investigate pentagon chain polymers (see Fig. 1) by a general multi-band Hubbard model where the electrons experience local Coulomb interactions on all lattice sites. The microscopic parameters are chosen such that they account for the particular environment and type of atom in the unit cell of the material; in particular, in our approach repulsive on-site interactions are permitted to differ on individual sites. Similarly, we also include bond dependent hopping amplitudes. The hopping parameters are not assumed to take special values leading to flat bands in the bare band structure. By contrast we will show rigorously that the dispersion of the correlated system may be *tuned by the interaction* to become flat. Thereby transitions to ferromagnetic states or correlated half-metallic states at high electron densities may be induced. We thus prove by exact means the conjecture of Brocks *et al.* [16] that the Coulomb interaction is able to stabilize magnetic order in acene and thiophene.

Our analytic approach proceeds in three steps: the transformation of the Hamiltonian into positive semidefinite form, the construction of ground states, and the proof of their uniqueness. This technique is independent of the spatial dimension and does not require integrability of the model. Previously it was successfully applied to construct exact ground states for Hubbard chains with other geometrical structures [17] and even for the three-

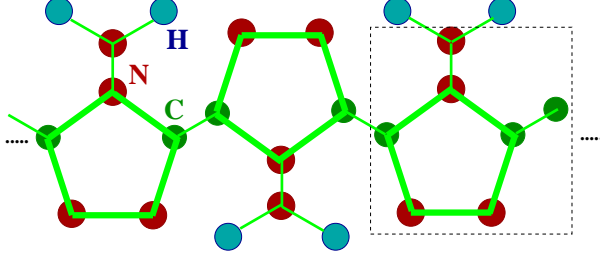


FIG. 1: (Color online) Schematic view of the pentagon-chain polymer polymethylaminotriazole. The dotted square indicates the cell presented in detail in Fig. 2.

dimensional periodic Anderson model [18]. Details of the method are described in Ref. [17].

Since the analytic technique employed here is applicable to a large class of chains we discuss it in its general form, and then specify it to a model analysis of the organic pentagon chain shown in Fig. 1. The unit cell contains $m = m_p + m_e \geq 2$ sites where m_p is the number of sites in the closed polygon as indicated in Fig. 2. In this case $m_p=5$, and $m_e = 1$ is the number of sites in the side groups; the number m (here $m = 6$) also determines the number of sublattices. The i -th unit cell then contains the sites $\mathbf{i} + \mathbf{r}_n$, $n \leq m$, with $\mathbf{r}_1 = \mathbf{0}$ and $\mathbf{r}_{m+1} = \mathbf{a}$; here $|\mathbf{a}|$ is the lattice constant. Altogether the chain consists of N_c cells, where neighboring cells connect through the single point \mathbf{r}_{m+1} . Subsequently we use periodic boundary conditions and fix the number of electrons to $N \leq N_\Lambda$, where $N_\Lambda = mN_c$ is the number of sites. The filling is denoted by $\rho = N/2N_\Lambda \leq 1$. In the following $\sum_{\mathbf{i}}$, $\prod_{\mathbf{i}}$ (or $\sum_{\mathbf{k}}$, $\prod_{\mathbf{k}}$ in momentum representation) mean sums and products, respectively, over the N_c cells.

The Hamiltonian we choose to describe the polymer chain has the form $\hat{H} = \hat{H}_0 + \hat{H}_U$ with

$$\hat{H}_0 = \sum_{\sigma, \mathbf{i}} \sum_{n, n' (n > n')} (t_{n, n'} \hat{c}_{\mathbf{i} + \mathbf{r}_n, \sigma}^\dagger \hat{c}_{\mathbf{i} + \mathbf{r}_{n'}, \sigma} + H.c.) + \sum_{\sigma, \mathbf{i}} \sum_{n=1}^m \epsilon_n \hat{n}_{\mathbf{i} + \mathbf{r}_n, \sigma}, \quad (1a)$$

$$\hat{H}_U = \sum_{\mathbf{i}} \sum_{n=1}^m U_n \hat{n}_{\mathbf{i} + \mathbf{r}_n, \uparrow} \hat{n}_{\mathbf{i} + \mathbf{r}_n, \downarrow}. \quad (1b)$$

Here $\hat{c}_{\mathbf{j}, \sigma}^\dagger$ creates an electron with spin σ at site \mathbf{j} , $t_{n, n'}$ are hopping matrix elements connecting the sites $\mathbf{i} + \mathbf{r}_{n'}$ and $\mathbf{i} + \mathbf{r}_n$. Furthermore, ϵ_n and $U_n > 0$ are on-site potentials and on-site

Coulomb interactions, respectively, defined at the sites $\mathbf{i} + \mathbf{r}_n$. The Fourier transform of $\hat{c}_{\mathbf{i}+\mathbf{r}_n,\sigma}$ will be denoted by $\hat{c}_{n,\mathbf{k},\sigma}$. We note that the Hamiltonian parameters are arbitrary at this point, i.e., they are not chosen to provide flat bands in the bare band structure. The case $\epsilon_n = 0$ for all n leaves the results qualitatively unchanged.

In the first step, we define $m - 1$ block operators $\hat{G}_{\alpha,\mathbf{i},\sigma}^\dagger = \sum_{\ell \in \mathcal{B}_{\mathbf{i},\alpha}} a_{\alpha,\ell} \hat{c}_{\mathbf{i}+\mathbf{r}_\ell,\sigma}^\dagger$ with $\alpha = 1, \dots, m - 1$, i.e., linear superpositions of creation operators acting on blocks $\mathcal{B}_{\mathbf{i},\alpha}$ consisting of the m sites $\mathbf{i} + \mathbf{r}_\ell$ in the unit cell at \mathbf{i} ; here $a_{\alpha,\ell}$ are numerical coefficients. Specifically for the pentagon cell shown in Fig. 2 we employ 3 three-site blocks (the triangles made of sites (1,2,5), (2,3,5), (3,4,5)), and 2 two-site blocks (the site pairs (5,6), (4,7)) [19]. The interaction term \hat{H}_U is rewritten in terms of the operators $\hat{P}_n = \sum_{\mathbf{i}} \hat{P}_{\mathbf{i}+\mathbf{r}_n}$, where $\hat{P}_{\mathbf{j}} = \hat{n}_{\mathbf{j},\uparrow} \hat{n}_{\mathbf{j},\downarrow} - (\hat{n}_{\mathbf{j},\uparrow} + \hat{n}_{\mathbf{j},\downarrow}) + 1$ is a positive semidefinite operator with eigenvalue zero when there is at least one electron on site \mathbf{j} . Altogether $\hat{H} - C_g$ takes the positive semidefinite form $\hat{H} - C_g = \hat{H}_G + \hat{H}_P$, where

$$\hat{H}_G = \sum_{\mathbf{i},\sigma} \sum_{\alpha=1}^{m-1} \hat{G}_{\alpha,\mathbf{i},\sigma} \hat{G}_{\alpha,\mathbf{i},\sigma}^\dagger, \quad \hat{H}_P = \sum_{n=1}^m U_n \hat{P}_n. \quad (2)$$

Here $C_g = q_U N - N_c [\sum_{n=1}^m U_n + 2 \sum_{\alpha=1}^{m-1} z_\alpha]$, $z_\alpha = \sum_{\ell} |a_{\alpha,\ell}|^2$, and q_U are constants which depend on the parameters entering in \hat{H} . The transformation of \hat{H} into the semidefinite form shown in Eq. (2) requires that the microscopic parameters in Eq. (1) fulfill certain conditions, i.e., equations connecting the coefficients $a_{\alpha,\ell}$ and q_U to the starting Hamiltonian parameters in Eq. (1). The solvability of the matching conditions determines the parameter space domain \mathcal{D} for which the transformation from Eq. (1) to Eq. (2) can be performed. It is not difficult to show that \mathcal{D} is not strongly restricted by the Hamiltonian parameters in Eq. (1). In particular, the values of the interaction parameters U_n can vary over a wide range. Details regarding the form of the matching conditions, the domain \mathcal{D} , and the block operators $\hat{G}_{\alpha,\mathbf{i},\sigma}^\dagger$ in Eq. (2) are presented in the Appendix.

Before we construct ground states of Eq. (2) above half filling ($\rho > 1/2$) we analyze its effective band structure. This is possible because the anticommutation relations for the composite block operators $\hat{G}_{\alpha,\mathbf{i},\sigma}^\dagger$, which depend on the interactions U_n , allow us to rewrite the operator \hat{H}_G as $\hat{H}_G = \hat{H}_{kin} + K_G$, with a kinetic energy operator $\hat{H}_{kin} = -\sum_{\mathbf{i},\sigma} \sum_{\alpha=1}^{m-1} \hat{G}_{\alpha,\mathbf{i},\sigma}^\dagger \hat{G}_{\alpha,\mathbf{i},\sigma}$ and a constant $K_G = 2N_c \sum_{\alpha=1}^{m-1} z_\alpha$. The kinetic part, \hat{H}_{kin} , is quadratic in the original fermionic operators $\hat{c}_{\mathbf{i}+\mathbf{r}_n,\sigma}$ and can hence be diagonalized, leading to an effective, interaction dependent band structure. In fact, the dispersion rela-

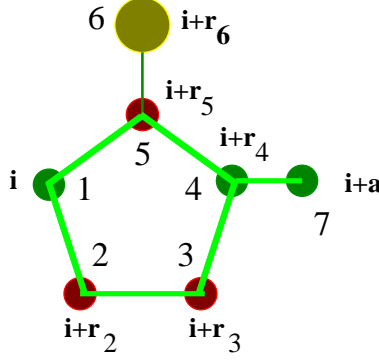


FIG. 2: (Color online) The pentagon cell with $m_p = 5$ and $m_e = 1$. The numbers indicate the index n of the site, \mathbf{a} is the primitive translation vector, and $\mathbf{i} + \mathbf{r}_n$ specifies the site position inside the cell.

tions thereby obtained are identical to the energy bands of \hat{H}_0 in Eq. (1b), but the on-site potentials ϵ_n are now replaced by the renormalized energies

$$\epsilon_n^R = \epsilon_n + U_n - qU. \quad (3)$$

It is this renormalization which can lead to an effective upper flat band. In the ground state $|\Psi_g\rangle$ of \hat{H} with $(\hat{H}_G + \hat{H}_P)|\Psi_g\rangle = 0$ (see below), this flatness is unaffected by the presence of \hat{H}_P in Eq. (2) since $\hat{H}_P|\Psi_g\rangle = 0$.

Thus we find the very remarkable result that a dispersive band structure of noninteracting electrons can be tuned by an interaction to yield an effective upper flat band of the interacting, many-electron system; an example is given Fig. 3 for a selected parameter set. The effectively flat band is half filled for the total number of particles $N = 2N_\Lambda - N_c \equiv N^*$, and is more than half filled for $N > N^*$. Such an interaction induced upper flat band is possible only if the local interactions U_n differ on at least one site in the unit cell. We note that properties of the exact ground state can only be deduced for the states in the upper band, the physics of the lower bands is not accessible by the here applied method (as indicated by the question mark in Fig. 3b).

The ground state for $N = N^$:* In this case the ground state of Eq. (2) has the form

$$|\Psi_g(N^*)\rangle = \left[\prod_{\sigma} \hat{G}_{\sigma}^{\dagger} \right] \hat{F}^{\dagger} |0\rangle, \quad (4)$$

where $|0\rangle$ is the vacuum state, $\hat{G}_{\sigma}^{\dagger} = \prod_{\mathbf{i}} \prod_{\alpha=1}^{m-1} \hat{G}_{\mathbf{i},\alpha,\sigma}^{\dagger}$, and the operator $\hat{F}^{\dagger} = \prod_{\mathbf{i}} \hat{c}_{\mathbf{i}+\mathbf{r}_{n_i},\sigma}^{\dagger}$ introduces one electron with spin σ in each unit cell. Since $\hat{G}_{\sigma}^{\dagger}$ creates $(m-1)N_c$ electrons

with spin σ , the state $|\Psi_g(N^*)\rangle$ contains $N_\sigma = mN_c$ electrons with spin σ . Therefore there is one σ electron on each site. Consequently all σ electrons are localized, and only the $-\sigma$ electrons are mobile. Therefore Eq. (4) may be identically rewritten as

$$|\Psi_g(N^*)\rangle = \prod_{\mathbf{i}} \left[\left(\prod_{n=1}^m \hat{c}_{\mathbf{i}+\mathbf{r}_n, \sigma}^\dagger \right) \left(\prod_{\alpha=1}^{m-1} \hat{G}_{\alpha, \mathbf{i}, -\sigma}^\dagger \right) \right] |0\rangle. \quad (5)$$

This state describes a half-metal, i.e., a non-saturated ferromagnet with total spin $S = N_c/2$. Eq. (4) is indeed the ground state since $\hat{H}_G|\Psi_g(N^*)\rangle = 0$ and $\hat{H}_P|\Psi_g(N^*)\rangle = 0$, where the former relation is due $(\hat{G}_{\alpha, \mathbf{i}, \sigma}^\dagger)^2 = 0$, while the latter is a consequence of $N_\sigma = N_\Lambda$. Since every site is occupied by an electron with spin σ that part of the wave function which describes the $-\sigma$ electrons is equivalent to a Slater determinant.

The spatial extension of the electrons with spin $-\sigma$ is obtained from the long-distance ($r \rightarrow \infty$) behavior of the ground-state expectation value of the hopping term $\Gamma_{\mathbf{i}}(\mathbf{r}) = \langle \Psi_g(N^*) | (\hat{c}_{\mathbf{i}+\mathbf{r}_n, -\sigma}^\dagger \hat{c}_{\mathbf{i}+\mathbf{r}_n+\mathbf{r}, -\sigma} + H.c.) | \Psi_g(N^*) \rangle$ for arbitrary $n = 1, \dots, m$. Explicit calculations yield an exponential decay of $\Gamma_{\mathbf{i}}(\mathbf{r})$ in the thermodynamic limit ($N_c \rightarrow \infty$). Hence the ferromagnetic state Eq. (5) is localized. Apart from the trivial $(2S + 1)$ degeneracy related to the orientation of the total spin, where $S = S_z^{Max} = N_c/2$, the ground state [20] is unique; this was proved by us using the technique presented in detail in Ref. [17].

The ground state for $N > N^$:* Here we restrict ourselves to the $S_z = S_z^{Max}$ sector. If we add \bar{N} electrons to the system these electrons can occupy only $-\sigma$ spin states. The ground state then has the form

$$|\Psi_g(N^* + \bar{N})\rangle = \hat{Q}_{\bar{N}}^\dagger |\Psi_g(N^*)\rangle, \quad (6)$$

where the operator $\hat{Q}_{\bar{N}}^\dagger = [\prod_{\gamma=1}^{\bar{N}} \hat{c}_{n_\gamma, \mathbf{k}_\gamma, -\sigma}^\dagger]$ is a product of \bar{N} arbitrary, but different, $\hat{c}_{n, \mathbf{k}, -\sigma}^\dagger$ operators. That Eq. (6) is indeed a ground state follows from the fact that $\hat{G}_{\alpha, \mathbf{i}, \sigma}^\dagger$ anticommutes with the fermionic creation operators $\hat{c}_{n, \mathbf{k}, -\sigma}^\dagger$ and hence also with the operators in $\hat{Q}_{\bar{N}}^\dagger$. Due to the free electrons with spin $-\sigma$ introduced by $\hat{Q}_{\bar{N}}^\dagger$ the ground state Eq. (6) contains also electrons in plane-wave like states. Furthermore, since $E_g = C_g$, one finds a vanishing charge excitation gap $\delta\mu = E_g(N + 1) - 2E_g(N) + E_g(N - 1) = 0$ for $\bar{N} > 1$.

In order to verify the extended character of the ground state Eq. (6) we calculate again the expectation value of the hopping term $\Gamma_{\mathbf{i}}(\mathbf{r}) = \langle \Psi_g(N^* + \bar{N}) | \hat{c}_{\mathbf{i}+\mathbf{r}_2, -\sigma}^\dagger \hat{c}_{\mathbf{i}+\mathbf{r}_2+\mathbf{r}, -\sigma} + H.c. | \Psi_g(N^* + \bar{N}) \rangle$ specifically for $\bar{N} = 1$ and $\hat{Q}_1 = \hat{c}_{2, \mathbf{k}^{(1)}, -\sigma}^\dagger$, where $\mathbf{k}^{(1)}$ is the arbitrary momentum of the

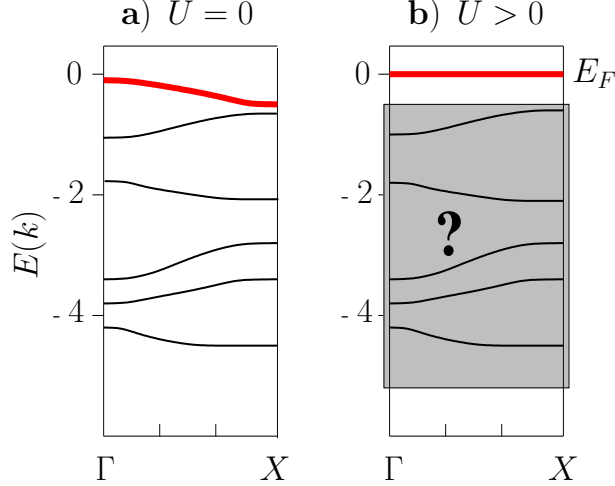


FIG. 3: (Color online) Dispersion of the pentagon polymer chain. a) Bare band structure (for details see the Appendix) for hopping parameters $t_c \equiv t_{4,7} = 0.5$, $t_h \equiv t_{3,2} = -1.1$, $t_f \equiv t_{5,6} = 1.2$, and on-site potentials $\epsilon_1 = \epsilon_4 = -2.5$, $\epsilon_2 = \epsilon_3 = -2.0$, $\epsilon_5 = -2.1$, $\epsilon_6 = -2.1$, using the site notation from Fig. 2. b) In the interacting case with the local interactions $U_1 = U_4 = 0.18$, $U_2 = U_3 = 0.35$, $U_5 = U_6 = 0.03$ and the same \hat{H}_0 parameters as in a). The upper band, indicated by a thick line, is determined by Eq. (3). Since $E(k)$ is even in $k = \mathbf{k} \cdot \mathbf{a}$, only $k \in [0, \pi]$ is shown. The question mark in the shaded area indicates that the exact behavior in this region is not known. All energies are in units of $t \equiv t_{2,1} = t_{1,5} = t_{5,4} = t_{4,3}$, with $t > 0$.

electron added above $N = N^*$. In the thermodynamic limit of the pentagon chain the result is

$$\Gamma_{\mathbf{i}}(\mathbf{r}) = \Gamma_0(\mathbf{r})(1 - A(\mathbf{k}^{(1)})/B(\mathbf{k}^{(1)})). \quad (7)$$

Here $\Gamma_0(\mathbf{r})$ is the plane-wave result for a free electron in a Bloch state, $A(\mathbf{k}) = A_1 + A_2 \cos \mathbf{k} \cdot \mathbf{a}$, and $B(\mathbf{k}) = B_1 + B_2 \cos \mathbf{k} \cdot \mathbf{a} > 0$ holds for all \mathbf{k} with constants A_1 , A_2 and B_1 , B_2 (for details see the Appendix). This shows that the localization length is indeed infinite.

For pentagon chains without external links (i.e., when the sites $\mathbf{i} + \mathbf{r}_6$ and $\mathbf{i} + \mathbf{r}_7$ in Fig. 2 are missing) the same solutions are found, but the regions of parameter space where they exist are shifted.

We emphasize that in the case of Mielke-Tasaki ferromagnetism, i.e., flat-band ferromagnetism in a half-filled lowest flat band [12], both the flat band and the connectivity conditions (the overlap of the local Wannier functions) necessary for the emergence of this type of ferromagnetism, result from the *bare* band structure determined by \hat{H}_0 . By con-

trast, we have shown here that the *interaction* may be employed to tune a fully dispersive bare band structure to become partially flat. The results apply to the high-density region where Brocks *et al.* conjectured the presence of strong correlations in acene and thiophene organic molecular crystals and the stabilization of magnetic phases [16]. Using the \hat{H}_0 parameters from Fig. 3, the matching conditions provide for the upper (bare) band a width of $W/t = 0.15$, with $0.2 \leq U_n/W \leq 2.3$. For other parameters in \hat{H}_0 the parameter space domain \mathcal{D} (see the Appendix) allows for even higher values of U_n/W .

Regarding the experimental realization of the ferromagnetic and the half-metallic states derived above we note that the required electron doping of the pentagon chains can, in principle, be achieved [21] by two means: first by raising the Fermi level by selecting appropriate side groups, and second by field-effect doping in a double-layer transistor structure [22]. Specifically for polythiophene with an estimated density of 10^{14} pentagon rings/cm² [23], electron densities of the order $10^{15} - 10^{16}$ carriers/cm² are required. As already verified these electron densities are experimentally achievable [24].

In summary, by employing a rigorous analytic method we have constructed exact ground states for a multiorbital pentagon Hubbard chain. The ferromagnetism and the half-metallicity of the derived solutions originate from an unexpected mechanism in multiorbital polygon chains with different site-dependent Coulomb interaction strengths. For high electron densities with the top band at least half-filled the interactions are capable of turning this dispersive band into an effectively flat band in an extended parameter region. The obtained solutions therefore point to a new route for the design of ferromagnetic pentagon-chain polymers.

Acknowledgements. We acknowledge valuable discussions with Wolfgang Brütting on organic materials and with Michael Sekania on exact diagonalization results. Support by the Alexander von Humboldt Foundation, the TAMOP 4.2.1.-08/1-2008-003 research project of EC at the University of Debrecen, and the Deutsche Forschungsgemeinschaft through SFB 484 in 2009 and TRR 80 as of January 1, 2010, is gratefully acknowledged.

[1] A. J. Heeger, S. Kivelson, J. R. Schrieffer, and W. P. Su, *Rev. Mod. Phys.* **60**, 781 (1988).

[2] A. S. Dhot, G. M. Wang, D. Moses, and A. J. Heeger, *Phys. Rev. Lett.* **96**, 246403 (2006).

- [3] C. Tanase, E. J. Meijer, P. W. M. Blom, and D. M. de Leeuw, *Phys. Rev. Lett.* **91**, 216601 (2003).
- [4] A. C. R. Grayson, I. S. Choi, B. M. Tayler, P. P. Wang, H. Brem, M. J. Cima, and R. Langer, *Nature Mater.* **2**, 767 (2003).
- [5] R. McNeill, R. Siudak, J. H. Wardlaw, and D. E. Weiss, *Austr. Jour. Chem.* **16**, 1056 (1963).
- [6] J. W. van der Horst, P. A. Bobbert, and M. A. J. Michels, *Phys. Rev. Lett.* **83**, 4413 (1999).
- [7] O. R. Nascimento, A. J. A. de Oliveira, A. A. Correa, L. O. S. Bulhoes, E. C. Pereira, V. M. Souza, and L. Walmsley, *Phys. Rev. B* **67**, 144422 (2003).
- [8] S. Majumdar, H. Majumdar, J. O. Lill, J. Rajander, R. Laiho, and R. Osterbacka, preprint arXiv:0905.2021.
- [9] F. R. de Paula, L. Walmsley, E. C. Pereira and A. J. A. de Oliveira, *J. Magn. Magn. Mater.* **320**, e193 (2008); A. A. Correa, L. Walmsley, L. O. S. Bulhoes, W. A. Ortiz, A. J. A. de Oliveira, and E. C. Pereira, *Synth. Met.* **121**, 1836 (2001).
- [10] Y. Suwa, R. Arita, K. Kuroki, and H. Aoki, *Phys. Rev. B* **68**, 174419 (2003).
- [11] R. Arita, Y. Suwa, K. Kuroki, and H. Aoki, *Phys. Rev. Lett.* **88**, 127202 (2002); *Phys. Rev. B* **68**, 140403(R) (2003).
- [12] A. Mielke and H. Tasaki, *Commun. Math. Phys.* **158**,341 (1993).
- [13] Y. Suwa, R. Arita, K. Kuroki, and H. Aoki, preprint arXiv:0907.2477.
- [14] C. D. Batista, J. Bonca, and J. E. Gubernatis, *Phys. Rev. B* **68**, 214430 (2003).
- [15] A. G. Petukhov, I. I. Mazin, L. Chioncel, and A. I. Lichtenstein, *Phys. Rev. B* **67**, 153106 (2003).
- [16] G. Brocks, J. van den Brink, and A. F. Morpurgo, *Phys. Rev. Lett.* **93**, 146405 (2004).
- [17] Z. Gulácsi, A. Kampf, and D. Vollhardt, *Phys. Rev. Lett.* **99**, 026404 (2007); *Progr. Theor. Phys. Suppl.* **176**, 1 (2008).
- [18] Z. Gulácsi and D. Vollhardt, *Phys. Rev. Lett.* **91**, 186401 (2003); *Phys. Rev. B* **72**, 075130 (2005).
- [19] A similar strategy with qualitatively similar results can be applied for arbitrary polygons with m_p sites in the polygon and m_e sites in side groups; in this case there are $m_p - 2$ three-site and $m_e + 1$ two-site blocks, leading to $m - 1$ block operators.
- [20] We note that Eq. (4) describes only the case of maximal spin projection S_z^{Max} . The ground states in the other spin sectors $S_z = N_c/2 - \bar{n} < S_z^{Max}$ are $|\Psi_g(N^*, \bar{n})\rangle = (\hat{S}_-)^{\bar{n}}|\Psi_g(N^*)\rangle$, where

$\hat{S}_- = \sum_{n=1}^m \sum_{\mathbf{i}} \hat{S}_-(\mathbf{i} + \mathbf{r}_n)$, $\hat{S}_-(\mathbf{i}) = \hat{c}_{\mathbf{i},\downarrow}^\dagger \hat{c}_{\mathbf{i},\uparrow}$, $\bar{n} = 1, \dots, N_c$. Since $\hat{P}_1 \hat{S}_-(\mathbf{i}') = \hat{S}_-(\mathbf{i}') \hat{P}_1 (1 - \delta_{\mathbf{i},\mathbf{i}'})$, $\hat{G}_{\alpha,\mathbf{i},\sigma}^\dagger \hat{S}_- = -\hat{G}_{\alpha,\mathbf{i},-\sigma}^\dagger \delta_{\sigma,\uparrow} + \hat{S}_- \hat{G}_{\alpha,\mathbf{i},\sigma}^\dagger$, $|\Psi_g(N^*, \bar{n})\rangle$ remains in the ground-state manifold.

- [21] A. Opitz, M. Kraus, M. Bronner, J. Wagner, and W. Brütting, *New J. Phys.* **10**, 065006 (2008).
- [22] K. Ueno, S. Nakamura, H. Shimotani, A. Ohtomo, N. Kimura, T. Nojima, H. Aoki, Y. Iwasa, and M. Kawasaki, *Nat. Mater.* **7**, 855 (2008); H. Yuan, H. Shimotani, A. Tsukazaki, A. Ohtomo, M. Kawasaki, and Y. Iwasa, *Adv. Funct. Mater.* **19**, 1046 (2009).
- [23] M. J. Panzer and C. D. Frisbie, *Adv. Funct. Mater.* **16**, 1051 (2006); H. Shimotani, G. Diguët, and Y. Iwasa, *Appl. Phys. Lett.* **86**, 022104 (2005).
- [24] M. J. Panzer and C. D. Frisbie, *J. Am. Chem. Soc.* **127**, 6960 (2005).

APPENDIX

1. DETAILS REGARDING THE TRANSFORMED HAMILTONIAN, EQ. (2), FOR THE PENTAGON CHAIN

a) The parameters of the transformed Hamiltonian, Eq.(2), obey the matching conditions

$$\begin{aligned} \sum_{\alpha=1}^{m-1} z_\alpha &= 4Q_1 + Q_1^2/|t_h| + 2t^2/Q_1 + 2(|t_h| + |t_c|) + Q_3^2 + t_f^2/Q_3^2, \\ q_U &= (1/2)[(U_1 + \epsilon_1 + |t_c|) + (U_2 + \epsilon_2 + |t_h|) + \{(U_2 + \epsilon_2 + |t_h|) - (U_1 + \epsilon_1 + |t_c|)\}^2 + 4t^2]^{1/2}, \\ Q_1 &= q_U - U_2 - \epsilon_2 - |t_h|, \quad Q_2 = q_U - U_1 - \epsilon_1 - |t_c|, \\ Q_3 &= |t_f| \sqrt{|t_h|} / [|t_h|(q_U - U_5 - \epsilon_5) - (q_U - U_2 - \epsilon_2)^2 + t_h^2]^{1/2}, \end{aligned} \quad (A1)$$

where $Q_1, Q_2, Q_3 > 0$, and the hopping amplitudes t, t_h, t_c, t_f are defined in the caption of Fig. 3.

b) The parameter space domain \mathcal{D} for which the transformation from Eq.(1) to Eq.(2) is valid is determined by the relations:

$$\begin{aligned} t_h &< 0, \quad Z = (q_U - Q_3^2) > \epsilon_6, \\ W &= q_U - [(q_U - U_2 - \epsilon_2)^2 - t_h^2]/|t_h| > \epsilon_5, \\ W - \epsilon_5 &> U_5 > 0, \quad U_6 = Z - \epsilon_6. \end{aligned} \quad (A2)$$

c) The block operators entering in the transformed Hamiltonian, Eq.(2), are given by the relations

$$\begin{aligned}
\hat{G}_{1,\mathbf{i},\sigma} &= q_S \hat{b}_{\mathbf{i},5,2} - t/q_S \hat{c}_{\mathbf{i}+\mathbf{r}_1,\sigma}, \\
\hat{G}_{2,\mathbf{i},\sigma} &= -t_S \hat{b}_{\mathbf{i},2,3} + Q_1 \hat{c}_{\mathbf{i}+\mathbf{r}_5,\sigma}/t_S, \\
\hat{G}_{3,\mathbf{i},\sigma} &= q_S \hat{b}_{\mathbf{i},5,3} - t/q_S \hat{c}_{\mathbf{i}+\mathbf{r}_4,\sigma}, \\
\hat{G}_{4,\mathbf{i},\sigma} &= Q_3 \hat{c}_{\mathbf{i}+\mathbf{r}_6,\sigma} - t_f/Q_3 \hat{c}_{\mathbf{i}+\mathbf{r}_5,\sigma}, \\
\hat{G}_{5,\mathbf{i},\sigma} &= |t_c|^{1/2} [\hat{c}_{\mathbf{i}+\mathbf{r}_4,\sigma} - t_c \hat{c}_{\mathbf{i}+\mathbf{a},\sigma}/|t_c|],
\end{aligned} \tag{A3}$$

where the notation $q_S = Q_1^{1/2}$, $t_S = |t_h|^{1/2}$, $\hat{b}_{\mathbf{i},n,m} = \sum_{p=n,m} \hat{c}_{\mathbf{i}+\mathbf{r}_p,\sigma}$ was used.

2. DISPERSION OF THE BARE BANDS OF THE PENTAGON CHAIN PRESENTED IN FIG. 3A

The energy of the bare bands presented in Fig. 3a, $\epsilon = E_\nu(k)$, $\nu \leq m$, is provided by the equation

$$\begin{aligned}
2t_c t^2 [(\epsilon_6 - \epsilon) T_h - t_h T_f] \cos k + T_f \{t_h^2 t_c^2 - (\epsilon_2 - \epsilon)^2 t_c^2 + [(\epsilon_1 - \epsilon)(\epsilon_2 - \epsilon) - t^2]^2 - (\epsilon_1 - \epsilon)^2 t_h^2\} \\
+ 2(\epsilon_6 - \epsilon) t^2 \{t^2 (\epsilon_2 + t_h - \epsilon) - (\epsilon_1 - \epsilon) T_h\} = 0,
\end{aligned} \tag{A4}$$

where $T_h = (\epsilon_2 - \epsilon)^2 - t_h^2$, $T_f = (\epsilon_6 - \epsilon)(\epsilon_5 - \epsilon) - t_f^2$, and $k = \mathbf{k} \cdot \mathbf{a}$.

3. DETAILS REGARDING THE EXPECTATION VALUE OF THE HOPPING TERM $\Gamma_{\mathbf{i}}(\mathbf{r})$

The parameters entering in the $\Gamma_{\mathbf{i}}(\mathbf{r})$ expression from Eq.(7) are given by the relations

$$\begin{aligned}
A_1 &= 2|t_c| \{Q_3^2 [2Q_1^2 (2|t_n| + Q_1) + 2t^2 (Q_1 + |t_n|) + Q_1 (t^2 + 2Q_1^2) + (Q_1^4 + Q_1^2 t^2)/|t_n|] \\
&\quad + t_f^2/Q_3^2 [t^2 (|t_n| + Q_1) + Q_1^3 - (Q_1^4 + Q_1^2 t^2)/|t_n|]\}, \\
A_2 &= 2t_c t^2 [(|t_n| t_f^2)/Q_3^2 - 2Q_3^2 (Q_1 + |t_n|)], \\
B_1 &= 2|t_c| \{Q_3^2 [(2|t_n| + Q_1^2/|t_n|)(Q_1^2 + t^2) + (t^2 + 2Q_1^2)(|t_n| + 2Q_1)] + (|t_n| t^2 t_f^2)/Q_3^2\}, \\
B_2 &= 2t^2 t_c [(|t_n| t_f^2)/Q_3^2 - Q_3^2 (|t_n| + 2Q_1)],
\end{aligned} \tag{A5}$$

and one has $B_1 + B_2 \cos(k) > 0$ for all $k = \mathbf{k} \cdot \mathbf{a}$.